Segmental Dynamics of Dilute Polystyrene Chains in Miscible Blends and Solutions

T. R. Lutz,† Yiyong He,‡ and M. D. Ediger*

Department of Chemistry, University of Wisconsin—Madison, Madison, Wisconsin 53706

Received June 21, 2005; Revised Manuscript Received September 15, 2005

ABSTRACT: ^{2}H NMR relaxation time measurements have been used to investigate the segmental dynamics of polystyrene chains in six miscible polymer blends in the limit of low polystyrene concentration. These data are combined with previously reported results for the segmental dynamics of dilute polystyrene chains in four solvents. Polystyrene dynamics in these 10 hosts are strongly correlated with the glass transition temperature T_g of the host, but the dilute chain dynamics are not slaved to the host matrix dynamics. The Lodge−McLeish model, using a single value for the self-concentration $\phi_{self} = 0.35$, reasonably describes polystyrene segmental dynamics in all 10 hosts and also describes previously reported dynamics of dilute polyisoprene chains in four miscible blends. The dilute polystyrene segmental dynamics can be more accurately described if ϕ_{self} is allowed to depend on blending partner, with the resulting variation of ϕ_{self} from 0.14 to 0.48.

Introduction

Two decades of experimental work has shown that the properties of miscible polymer blends are more complex than those of undiluted homopolymers. For example, in contrast to homopolymer melts,[1−3] time−temperature superposition often fails dramatically when applied to the rheology of polymer blends,[4−8] and very broad blend glass transitions are typically observed.[5,6,9] It is generally accepted that these macroscopic observations are a result of distinct dynamics in miscible polymer blends.[10−12] Even though these blends are well-mixed on a molecular level, the dynamics of the individual components are not equal to each other and have their own temperature dependences.

To predict the macroscopic properties of polymer mixtures, an understanding of both the segmental and terminal dynamics of each component in the material is essential. Experimental[4−33] and simulation[34−37] work on miscible blends have led to the development of models that attempt to predict component dynamics.[33,38−46] Several of these models attempt to explain distinct component dynamics by considering the average composition around the segments of a given type of polymer. In this approach, if segments of polymer A are generally found in environments that are richer in A than the overall composition, then the dynamics of polymer A will be biased toward those of pure A. Two major mechanisms have been considered to be the source of this locally biased concentration. *Self-concentration* describes the effect that intramolecular connectivity has the local concentration; an A segment in the middle of a chain is guaranteed to have A segments attached to it on either side.[12,38−41] In addition, when the interaction parameter χ is greater than zero, the average local concentration of polymer A may be enhanced due to *intermolecular* composition fluctuations.[38,40,45] The extent to which average relaxation times are influenced by these two effects depends largely on the size of the local volume that controls the dynamics. If the relevant local volume is small, the self-concentration effect would be expected to be dominant.

Among the various models that attempt to predict distinct component dynamics, the Lodge−McLeish model[41] has received considerable attention recently.[18,20−23,29,47] In this approach only the self-concentration is considered, and the relevant local volume is assumed to be the Kuhn length at all temperatures and compositions; the self-concentration ϕ_{self} is calculated from the Kuhn length. When combined with the Fox equation, this model predicts the dynamics of the two components in a blend based only upon pure homopolymer properties. The predictions generated in this manner generally capture the qualitative trends of the experimental data but often are not quantitatively accurate.[21] As a result, ϕ_{self} has been used as a fitting parameter to describe a particular component with a particular blending partner. If the fitted ϕ_{self} values were found to strongly depend on many variables (temperature, composition, blending partner), that would likely mean that this approach is fundamentally incorrect (and not very useful practically). While a constant value of ϕ_{self} can describe many experimental data sets in which temperature[48−50] and composition are varied,[21] we have reported that the fitted value of ϕ_{self} can vary significantly with blending partner.[29]

In this paper, we examine critically the dependence of ϕ_{self} upon blending partner by comparing the dynamics of dilute polystyrene chains in 10 different blending partners. We have utilized dilute miscible blends[13,28,29,51] for two reasons. First, since a dilute chain is completely surrounded by chains of matrix polymer, these experiments maximize the influence of the blending partner on the dilute chain's dynamics. Second, in any given blend, the one phase region exists over a wider range of temperature at the edges of the phase diagram than in the middle. Thus, a larger range of blending partners can be explored in the one phase region if dilute blends are utilized.

The dilute species used in these experiments is backbone deuterated polystyrene. Deuterium NMR

† Present address: Stepan Company, 22 W. Frontage Road, Northfield, IL 60093.
‡ Present address: Department of Chemistry, University of Minnesota, Minneapolis, MN 55455.
* Corresponding author. E-mail: ediger@chem.wisc.edu.

10.1021/ma0513113 CCC: $30.25
Published on Web 10/22/2005

Table 1. Characterization of Homopolymers

polymer	M_n (g/mol)	M_w/M_n	T_g (K)	% d_3PS in blend
d_3-polystyrene (d_3PS)	1670	1.06	331	
poly(vinyl methyl ether)	46500	1.95	250	0.5, 2, 10
poly(vinyl ethylene)[a]	2500	1.04	248	2
polyisoprene[b]	3000	1.08	204	2
1,4-polybutadiene[c]	2300	1.05	177	2
h-polystyrene (PS15)	14800	1.03	369	2
poly(methyl methacrylate)	2200	1.14	336	2

[a] 89% 1,2-polybutadiene. [b] 81% *cis*-1,4, 14% *trans*-1,4, 5% 3,4. [c] 90% 1,4-polybutadiene.

techniques are well-developed and sensitive,[52,53] allowing the dynamics of dilute chains to be examined at concentrations as low as 0.5%.[28] We have studied the segmental dynamics of low molecular weight d_3-polystyrene (1670 g/mol) in host matrices of polybutadiene, polyisoprene, poly(vinylethylene), poly(vinyl methyl ether), poly(methyl methacrylate), and higher molecular weight polystyrene. We compare these results with previously published results on the segmental dynamics of 10% d_3-polystyrene (56 000 g/mol) in four solvents: toluene, *cis*-decalin, dioctyl phthalate, and dibutyl phthalate.[54]

The observed dynamics of polystyrene are well described by the Lodge−McLeish model with a single value of ϕ_{self} for a given host matrix; however, ϕ_{self} varies depending upon the identity of the host. We argue that a more insightful way to discuss these results is to compare the temperature shift of the dilute chain dynamics to the glass transition temperature of the host polymer or solvent. In this format, a single value of ϕ_{self} (0.35) reasonably describes the experimental data in all 10 hosts. We further show that this conclusion also extends to previously reported results for dilute polyisoprene chains. For these two systems (polyisoprene and polystyrene), we conclude that the Lodge−McLeish model provides useful predictions for segmental dynamics with a ϕ_{self} value that is independent of temperature, blending partner, and composition.

Experimental Methods

Materials. Backbone deuterium-enriched polystyrene (d_3-PS), M_n = 1670 g/mol, was purchased from Polymer Source, Inc., as were polyisoprene (PI), 1,4-polybutadiene (PB), poly(vinylethylene) (PVE), poly(methyl methacrylate) (PMMA), and polystyrene (PS15). Poly(vinyl methyl ether) (PVME) was obtained from Scientific Polymer Products, Inc. Characterization information for these polymers is given in Table 1.

Blend Preparation. Two-component dilute d_3PS miscible blends were prepared either by freeze-drying or by solvent-casting. d_3PS blends with PS15 and PMMA were prepared via freeze-drying from benzene solution, dilute blends with PI, PB, and PVE were solvent cast from dilute benzene solution, and PVME blends were solvent cast from tetrahydrofuran (THF).

The freeze-drying preparation technique employed here was previously described in detail.[28] For blends prepared via solvent casting, ~500 mg of total polymer was dissolved in 50 mL of either benzene or THF. This solution was placed on a glass surface, and solvent was removed under vacuum at room temperature for 48 h, after which the samples were heated at 343 K for 24 h. A final heat treatment under vacuum at 400 K for a minimum of 2 h was used to ensure complete removal of solvent. The resulting polymer blend film was ~1 mm thick. For blends with PI, PVE, and PB hosts, the samples were fluid and flowed easily at 300−340 K. These samples were transferred to NMR tubes via a pipet. The sample was then heated to allow the blend to flow to the bottom of the NMR tube and sealed under vacuum.

The d_3PS/PVME blends were extremely viscous and difficult to manipulate at room temperature. Furthermore, these dilute blends did not flow upon heating in the NMR tube. Because of these issues, a different method of transfer from the thin film to the NMR tube was used for d_3PS/PVME blends. These samples were cooled well into the glassy state by submersion in liquid nitrogen. Keeping the sample immersed in liquid nitrogen, the vial containing the blend was broken and the blend was carefully separated from the broken vial. Maintaining the glassy state, small pieces of the blend were transferred to an NMR tube. A homemade plunger was used to condense the polymer pieces as much as possible while the sample was allowed to warm to room temperature. The d_3PS/PVME blend was then placed under vacuum for 24 h, followed by heating to ~400 K for 10 min. After the sample cooled, the NMR tube was sealed under vacuum.

To ensure that these methods removed all solvent from the blends, two tests were performed. The thin film samples were heated under vacuum at high temperature until sample weight remained constant. This was taken as evidence that all solvent had been removed. A second, more rigorous test was performed on pure d_3PS. This sample was prepared via both freeze-drying and solvent casting from benzene solution as described above. The NMR measurements and DSC T_g values of pure d_3PS prepared via both methods were identical. Further, high molecular weight polystyrene yielded T_g values equal to 100 °C with both preparation methods, which is in agreement with the expectation that no solvent is present.

All d_3PS/host blends were studied at a composition of 2 wt % d_3PS. For some blends, additional samples containing 0.5 and 10 wt % d_3PS were prepared and characterized to check that the dilute regime had been reached.

***T_g* and Miscibility.** Differential scanning calorimetry thermograms were obtained using a Netzsch 200 DSC calibrated to a heating rate of 10 K/min using melting point standards. T_g was determined from four successive heating and cooling cycles at a rate of 10 K/min over temperatures ranging from T_g − 50 K to T_g + 50 K. The first heating cycle was used to erase thermal history while the final three traces, obtained immediately after cooling, were averaged to determine the homopolymer T_g values given in Table 1. Successive scans gave T_g values that agree to within 1 K.

For polymers with molecular weights similar to those used here, previous work has shown blends of PS with PB,[55] PVE,[55] PI,[56,57] PVME,[58,59] and PMMA[60] to be miscible over the composition and temperature range relevant for this study. Optical clarity was taken as further evidence of blend miscibility. In d_3PS blends with PB, PVE, and PMMA no cloud point was observed. Cloud points were observed in 2% d_3PS blends with PI upon cooling (~280 K) and for blends with PVME upon heating(~500 K). All observed cloud points are outside the temperature range of this study.

NMR Measurements. ^{2}H spin−lattice relaxation (T_1) measurements were performed using the standard inversion recovery ($\pi-\tau-\pi/2$) pulse sequence. T_1 is the time required for the magnetization to return to its equilibrium state after an initial inversion. A three-parameter fit was used to determine T_1 using the peak area, after the data had been processed with line broadening equal to one-tenth the line width of the spectrum. On the basis of a minimum of three trials at each temperature, the uncertainty in T_1 is ±6%.

^{2}H NMR measurements were performed at two frequencies using two different NMR spectrometers: Varian Inova-500 NMR spectrometer (76.7 MHz) and Bruker DMX-300 (15.2 MHz). On both spectrometers, temperature was controlled to ±0.5 K and calibrated within ±2 K using an ethylene glycol thermometer and melting point standards. The low-temperature limit of the measurements was dictated by adequate ^{2}H signal intensity and line width. (Representative spectra are available as Supporting Information.) The high-temperature limit was either set by NMR spectrometer temperature limits or set to prevent PI degradation in the case of d_3PS/PI blends. After exposure to high temperature, T_1 was reacquired at lower temperatures as a test of sample degradation. In all cases, the

T_1 measurements after exposure to high temperatures agreed with earlier measurements to within experimental error.

Data Interpretation

NMR Relaxation Equations. T_1 relaxation of ^{2}H nuclear spins is dominated by electric quadrupole coupling and is directly related to reorientation of C−D bonds. The connection between C−D reorientation and the NMR observable T_1 is described below.

The spin−lattice relaxation time T_1 of deuterium can be written as

$$\frac{1}{T_1} = \frac{3}{10}\pi^2\left(\frac{e^2qQ}{h}\right)^2 [J(\omega) + 4J(2\omega)] \quad (1)$$

Here $\omega/2\pi$ is the Larmor frequency. The quadrupole coupling constant e^2qQ/h was taken as 172 kHz from literature values for d_3PS backbone deuterons.[61−64] In eq 1, $J(\omega)$ is the spectral density function and is the Fourier transform of the orientation autocorrelation function $G(t)$ for the C−D bond:

$$J(\omega) = \frac{1}{2}\int_{-\infty}^{\infty} G(t)e^{-i\omega t}\,dt \quad (2)$$

The autocorrelation function, $G(t)$, can be written as

$$G(t) = \frac{3}{2}\langle\cos^2\theta(t)\rangle - \frac{1}{2} \quad (3)$$

where $\theta(t)$ is the angle of the C−D bond relative to its orientation at time $t = 0$.

Correlation Function and Correlation Times. We use a modified Kohlrausch−Williams−Watts (mKWW) function for the orientation autocorrelation function

$$G(t) = a_{\text{lib}}e^{-t/\tau_{\text{lib}}} + (1 - a_{\text{lib}})e^{-(t/\tau_{\text{seg}})^{\beta}} \quad (4)$$

This function indicates that C−D vector reorientation occurs via two mechanisms: librational and segmental motions. In this equation, a_{lib} and τ_{lib} are the amplitude and relaxation time for librational motion; τ_{lib} is set to 1 ps in our fitting analysis as the fit is insensitive to this value. The remaining two parameters in the equation, τ_{seg} and β, describe the characteristic segmental relaxation time as well as the distribution associated with it. Additionally, we assume τ_{seg} follows a Vogel−Tammann−Fulcher (VTF) temperature dependence (equivalent to WLF equation):[65,66]

$$\log\left(\frac{\tau_{\text{seg}}}{\tau_\infty}\right) = \frac{B}{T - T_0} \quad (5)$$

where τ_∞, B, and T_0 are constants for a given component in a particular blend. The correlation time for segmental dynamics $\tau_{\text{seg,c}}$ is the time integral of the segmental portion of the correlation function:

$$\tau_{\text{seg,c}} = \frac{\tau_{\text{seg}}}{\beta}\Gamma\left(\frac{1}{\beta}\right) \quad (6)$$

Equations 4−6 have previously been shown to give excellent agreement with experimental data[67,68] and molecular simulations.[64]

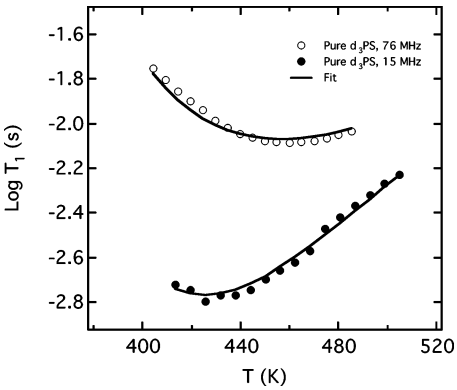

Figure 1. ^{2}H T_1 values for pure d_3PS obtained at 15 and 76 MHz. Solid lines show the fit obtained by simultaneously fitting all the data to eqs 1−5. Fit parameters are given in Table 2.

Table 2. Fit Parameters[a] for d_3PS Segmental Dynamics in the Melt, Blends, and Solutions

blend	B[a] (K)	T_0 (K)	a_{lib}	τ_∞ (ps)	β
pure d_3PS	454	295	0.15	1.6	0.47
0.5% d_3PS/PVME	454	252	0.12	1.4	0.49
2% d_3PS/PVME	454	252	0.12	1.5	0.49
10% d_3PS/PVME	454	255	0.15	1.5	0.49
2% d_3PS/PVE	454	233	0.17	1.4	0.51
2% d_3PS/PI	454	205	0.06	1.5	0.46
2% d_3PS/PB	454	185	0.09	1.9	0.49
2% d_3PS/hPS	454	324	0.31	1.7	0.47
2% d_3PS/PMMA	454	322	0.20	1.3	0.43
10% d_3PS56/DOP	454	205	0.22	3.5	0.65
10% d_3PS56/DBP	454	195	0.11	2.3	0.58
10% d_3PS56/decalin	454	166	0.13	2.5	0.58
10% d_3PS56/toluene	454	105	0.03	2.2	0.54

[a] B constrained to 454 K for all fits except pure d_3PS.

Results

Pure d_3PS Dynamics. NMR T_1 measurements were performed on the backbone deuterons of pure d_3PS over a broad temperature range and at two magnetic fields (^{2}H Larmor frequencies of 15 and 76 MHz). These results for pure d_3PS are presented in Figure 1. The best fit of the T_1 data with eqs 1−5 are shown as solid lines, and the fit parameters are given in Table 2. Since B and T_0 are strongly correlated over the temperature range of this study, the fit to pure d_3PS T_1 data was constrained such that $\tau_{\text{seg,c}} = 10$ s at the measured DSC T_g (331.4 K). With this constraint, the best fit to the pure d_3PS data was achieved with $B = 454$ K, and this fit is shown in Figure 1. The fit quality is indistinguishable from the best fit without any constraint (not shown).

The segmental correlation times for pure d_3PS (calculated using the parameters in Table 2 and eq 6) are shown in Figure 2 as the thick solid line. Representative error bars are also shown and were determined from the range of fits (including variations in B) that successfully described the measured T_1 values within experimental errors.

Dynamics of Dilute d_3PS in PVME. We have utilized blends containing 2% d_3PS and we argue here that these results fairly represent the limit of infinite dilution where the polystyrene dynamics are independent of composition. One way to define a dilute solution is by the overlap volume fraction $\phi^* = N\nu_0/[(4\pi/3)R_g^3]$,

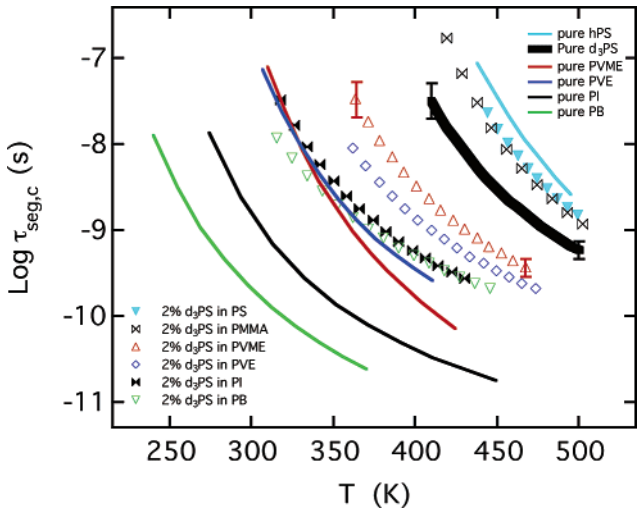

Figure 2. Segmental correlation times for miscible blend components. The segmental dynamics of dilute polymer chains are distinct from the dynamics of the host chains. The black solid line is the correlation time curve for pure d_3PS calculated using the fit parameters in Table 2. The symbols are the correlation times for 2% d_3PS in the blends. Solid lines show the segmental dynamics of pure host polymers. Representative error bars are shown.

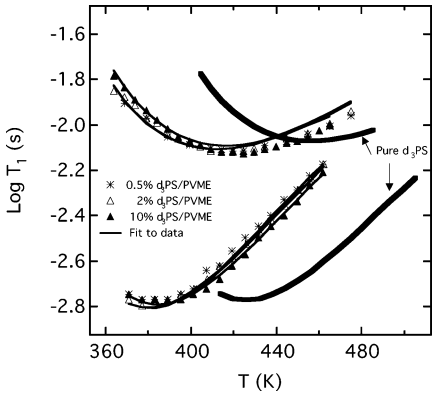

Figure 3. ^{2}H T_1 values for d_3PS in blends with PVME at d_3-PS at 15 and 76 MHz (lower and upper curves, respectively). Segmental dynamics at and below 10% d_3PS are nearly composition independent. Solid lines show the fits obtained for each composition by simultaneously fitting data from both fields. Fit parameters are given in Table 2. For comparison, the bold line shows the T_1 values for the pure d_3PS homopolymer (from Figure 1).

where N is the degree of polymerization and v_0 is the monomer volume. The overlap volume fraction of the d_3PS used here is $\phi^* \approx 0.4$, which indicates negligible chain overlap in the 2% blends. Further evidence supporting the infinite dilution interpretation comes from comparing ^{2}H NMR T_1 values for 0.5, 2, and 10% d_3PS in PVME, as shown in Figure 3. The T_1 values for d_3PS in these three blends are similar, while they are substantially different from the T_1 values for pure d_3-PS. A small change in d_3PS T_1 values is observed as the d_3PS concentration increases from 2% to 10%; this is expected when high-T_g chains are added to a low-T_g matrix. The very small changes in T_1 values of d_3PS between 0.5% and 2% d_3PS support our interpretation of 2% blends as being in the infinite dilution limit.

Comparing the segmental correlation times ($\tau_{seg,c}$) of d_3PS in 0.5, 2, and 10% blends with PVME provides a more rigorous test for the dilute limit. Before this comparison can be made, we will describe how $\tau_{seg,c}$ is

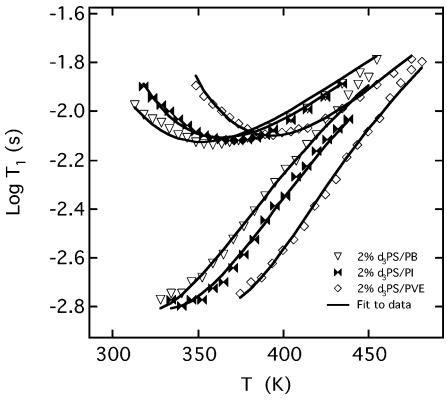

Figure 4. ^{2}H T_1 values for d_3PS in 2% blends with PB, PI, and PVE at 15 and 76 MHz (lower and upper curves, respectively). Solid lines show the fit obtained for each blend by simultaneously fitting data from both fields. Fit parameters are given in Table 2.

determined from the NMR T_1 data for all the dilute d_3-PS blends. The NMR T_1 data at both Larmor frequencies for a given blend was fit simultaneously using eqs 1−5 with the constraint that $B = 454$ K. It is important to note that the constraint on B does not impact the segmental correlation times reported here; all B and T_0 combinations that successfully fit the T_1 data produce correlation times consistent to those reported to within the error bars provided. The best fits to the T_1 values of d_3PS in PVME are presented as solid lines in Figure 3. The fit parameters are given in Table 2, and the correlation times for 2% d_3PS/PVME are presented in Figure 2.

The segmental correlation times of d_3PS in 0.5, 2, and 10% d_3PS/PVME blends are identical within experimental error, supporting the interpretation of 2% blends as representing the dilute limit. While pure d_3PS is more than 1 decade slower than d_3PS in a 2% d_3PS/PVME blend, the best fit $\tau_{seg,c}$ values for d_3PS in 0.5 and 2% d_3PS/PVME blends are within 0.03 decades, and the dynamics for 10% d_3PS in PVME are at most 0.15 decades slower than 2% d_3PS in PVME.

The fit quality presented in Figure 3 is reasonable although the fits are not perfect at high temperature. The data were fit under a variety of constraints that produced fits of comparable quality (for example, in some of these fits the high-temperature data were well described while deviations were seen at lower temperatures). On the basis of these fits, we are confident that the reported segmental correlation times of d_3PS in PVME presented in Figure 2 are accurate to within the reported error bars.

Dynamics of Dilute d_3PS in Other Low-T_g Hosts. The T_1 values for 2% d_3PS blended with PB, PI, and PVE are presented in Figure 4. The T_1 data were fit as described above, and the best fits are shown as solid lines in Figure 4. The fit parameters are listed in Table 2, and corresponding segmental correlation times are plotted in Figure 2. The fit quality for the T_1 data set of each of these blends is excellent.

Dynamics of Dilute d_3PS in High-T_g Hosts. The ^{2}H NMR T_1 results for 2% d_3PS/PS15 and 2% d_3PS/PMMA are given in Figure 5 along with best fits to the data. Fit parameters can be found in Table 2, and the corresponding correlation times for d_3PS in PS15 and PVME are given in Figure 2.

Dynamics of Dilute d_3PS in Solution. Previous work investigated the dynamics of 10% solutions of

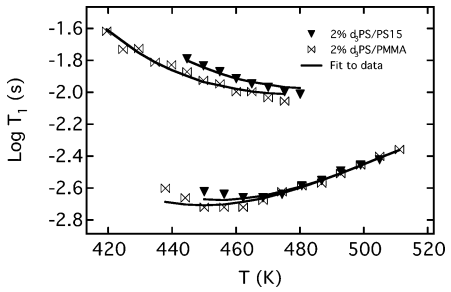

Figure 5. ^{2}H T_1 values for d_3PS in 2% blends with PMMA and PS15 at 15 and 76 MHz (lower and upper curves, respectively). Solid lines show the fit obtained for each blend by simultaneously fitting data from both fields. Fit parameters are given in Table 2.

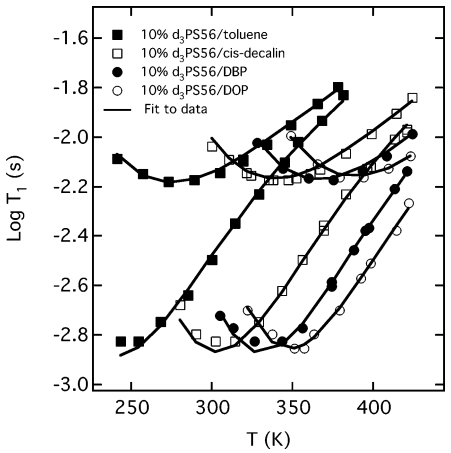

Figure 6. ^{2}H T_1 values for 10% d_3PS56 solutions in toluene, *cis*-decalin, dioctyl phthalate, and dibutyl phthalate at 15 and 76 MHz (lower and upper curves, respectively). The T_1 data are reproduced from ref 54. Solid lines show the fit obtained for each solution by simultaneously fitting data from both fields. Fit parameters are given in Table 2.

polystyrene in toluene, *cis*-decalin, dioctyl phthalate (DOP), and dibutyl phthalate (DBP).[54] ^{2}H NMR T_1 values were reported for a 56 kg/mol backbone ^{2}H-labeled polystyrene (d_3PS56) in the four solvent hosts. Since ref 54 predates the development of our current fitting approach, we have refit these data to obtain segmental correlation times. The 10% d_3PS56 solution T_1 values from ref 54 are reproduced in Figure 6. The best fit to each data set is presented as a solid line, and the resulting fit parameters can be found in Table 2. The corresponding $\tau_{seg,c}$ values are shown in Figure 7. Note that we report $\tau_{seg,c}$ here while τ_c is given in ref 54 (over a narrower temperature range). The τ_c values from the fits of eqs 1−5 and the τ_c values previously reported agree to within 0.04 decades (comparison not shown).

The low molecular weight d_3PS used in the present work has a glass transition temperature that is 40 K lower than the d_3PS56 used in ref 54. Because homopolymer d_3PS56 T_1 data have not been reported, the $\tau_{seg,c}$ values for pure d_3PS56 in Figure 7 are estimated on the basis of $\tau_{seg,c}$ values of the d_3PS used in this study. It has been shown that pure polystyrenes of different molecular weights have very similar segmental correlation times when compared at the same $T - T_g$.[64,69] Thus, $\tau_{seg,c}$ for d_3PS56 is taken to be equal to the $\tau_{seg,c}$ values of d_3PS determined here, shifted by 40 K (ΔT_g of d_3-PS56 and d_3PS). All subsequent analysis of d_3PS56/solution studies is performed using this estimate for pure d_3PS56 segmental correlation times.

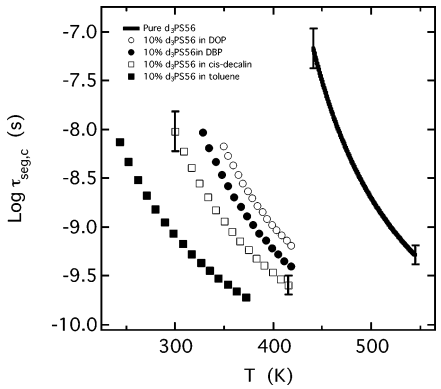

Figure 7. Segmental correlation times for pure d_3PS56 and for 10% d_3PS56 solutions in toluene, *cis*-decalin, dioctyl phthalate, and dibutyl phthalate. Curves and points were calculated using the fit parameters in Table 2.

Data Superposition. A model-independent analysis of the effect of blending on segmental dynamics can be made by directly superposing the blend and solution data onto the data for pure d_3PS. A master superposition plot of d_3PS T_1 values in all blends and solutions is given in Figure 8. Both temperature shifts (equal to $\Delta T_0 \pm 3$ K) and small vertical shifts (<0.08 in log T_1) were employed to yield the master curve. The resulting superposition is excellent. This means that, to a good approximation, the segmental dynamics of d_3PS in all blends and solutions are the same as the dynamics of pure d_3PS with a shift in temperature. This point will be discussed further below.

Discussion

We begin by commenting upon the general trends for dilute polystyrene segmental dynamics in polymer and solvent hosts, as shown in Figures 2 and 7. Qualitatively, the data are consistent with the idea that the glass transition temperatures (T_g) of the matrix controls the segmental dynamics. (See Table 1 and endnote[70] for T_g values.) When the host is a polymer of slower segmental dynamics [T_g(host) > T_g(d_3PS)], the d_3PS chains slow upon blending, as expected. When the host is a polymer of faster segmental dynamics or a solvent [T_g(host) < T_g(d_3PS)], the dilute d_3PS chains relax faster than in pure d_3PS. If all the segmental dynamics data in all the hosts is ordered, from fastest to slowest, this order coincides with an ordered list of host T_g values.

It is useful to compare the dynamics of the dilute d_3-PS chains to the dynamics of the host chains. The segmental dynamics of each host (as a pure homopolymer) are presented in Figure 2. Correlation times for the host polymer in the blend (98% host) should be very similar to those in the host homopolymer (100% host). The melt segmental dynamics are reproduced from literature values for PB,[22] PI,[29] PVE,[22] and PVME[29] with small temperature shifts to account for T_g differences.[71] Pure PMMA segmental correlation times are absent from Figure 2 because literature values determined via ^{13}C or ^{2}H NMR T_1 measurements could not be found.

Figure 2 shows clearly that the segmental dynamics of d_3PS in a dilute blend are distinct from the dynamics of its host for all blends studied. At any given temperature, the value of $\tau_{seg,c}$ of dilute d_3PS is different from that of its host, often separated by a factor of 10 or greater. Furthermore, the temperature dependence of $\tau_{seg,c}$ for the dilute d_3PS chains is likely different than

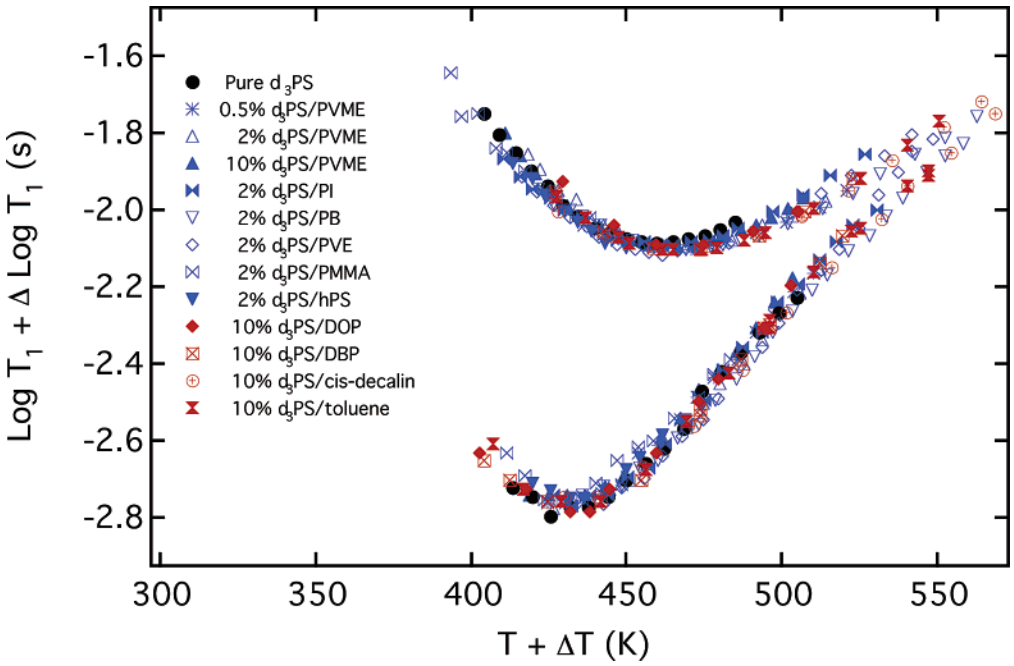

Figure 8. Superposition of the T_1 data for all d_3PS blends and solutions presented in Figures 1, 3, 4, 5, and 6. For each sample, a single horizontal and vertical shift suffices to simultaneously superpose the data at 15 and 76 MHz with the T_1 data for pure d_3PS.

that of its host, although given the error bars on the data we cannot make a definitive statement about this.

Lodge−McLeish Model. We next ask if the Lodge−McLeish (LM) model[41] is consistent with the measured segmental dynamics of dilute d_3PS in blends and solutions. The LM model assumes that the chemical composition of the region within one Kuhn length (l_K) of a given polymer segment determines the mobility of that segment. This local concentration (ϕ_{eff}) is calculated by considering the bulk concentration (ϕ) and the self-concentration (ϕ_{self}):

$$\phi_{eff} = \phi_{self} + (1 - \phi_{self})\phi \tag{7}$$

LM estimates the self-concentration ϕ_{self} as

$$\phi_{self} = \frac{C_\infty M_0}{k\rho N_{AV} V} \tag{8}$$

Here C_∞ is the characteristic ratio, M_0 is the repeat unit molar mass, k is the number of backbone bonds per repeat unit, ρ is the density, N_{av} is Avogadro's number, and $V = l_K^3$.

In this model, polymer segments of a given type have an effective glass transition temperature that is different from the macroscopic blend T_g because ϕ_{eff} differs from ϕ. In our implementation of the LM model,[18] we have used the Fox equation to calculate the effective T_g:

$$\frac{1}{T_g(\phi_{eff})} = \frac{\phi_{eff}}{T_{g,A}} + \frac{1 - \phi_{eff}}{T_{g,B}} \tag{9}$$

We predict segmental dynamics in the blend by correlating changes in $T_{g,eff}$ with changes in T_0

$$T_{0,i}(\phi) = T_{0,i} + [T_{g,i}(\phi) - T_{g,i}] \tag{10}$$

while assuming that the remaining VTF parameters (B, τ_∞) do not change with blending. One would anticipate that B for a homopolymer melt should depend on both intramolecular and intermolecular interactions. Thus, the assumption that B does not change upon blending is not necessarily correct and is particularly questionable in the dilute limit. Nevertheless, the data superposition presented in Figure 8 is reasonably consistent with this assumption; perfect superposition would imply that B is exactly independent of the environment of the d_3PS chains in the temperature range of our measurements.

Fits to the Lodge−McLeish Model. Figure 9 shows that all d_3PS segmental correlation times in dilute polymer blends and solutions can be well fit with the Lodge−McLeish model. The blue points in Figure 9 are the segmental correlation times of 2% d_3PS in polymer hosts, while the red points represent 10% d_3PS solutions. The dashed lines are the LM fits with ϕ_{self} as the single fitting parameter for each mixture; fit values are given in Table 3. Table 3 shows that the fitted values of ϕ_{self} depend on blending partner for d_3PS dynamics in polymer and solvent hosts.

Equation 8 predicts ϕ_{self} to be 0.27 for d_3PS, using C_∞ and ρ for bulk polystyrene at 410 K. C_∞ and l_K for polystyrene could potentially change with blending partner, but the changes in ϕ_{self} would be expected to be small.[29,72,73] Similarly, changes in ρ with temperature would have only a small influence on the prediction of eq 8, changing ϕ_{self} by at most 0.03. We therefore interpret the range of ϕ_{self} required to describe the experimental data as indicating a failure of eq 8. Lodge and McLeish recognized that eq 8 might need to be modified for specific polymers. Our finding extends beyond this suggestion and shows that ϕ_{self} must depend on blending partner in order to obtain quantitative fits to the data.

For the d_3PS/PMMA blend, we cannot determine a physically meaningful ϕ_{self} value. The T_g values of the PMMA and d_3PS homopolymers used are nearly identical, and consequently the LM model predicts the $\tau_{seg,c}$ values of d_3PS in PMMA will be essentially identical to

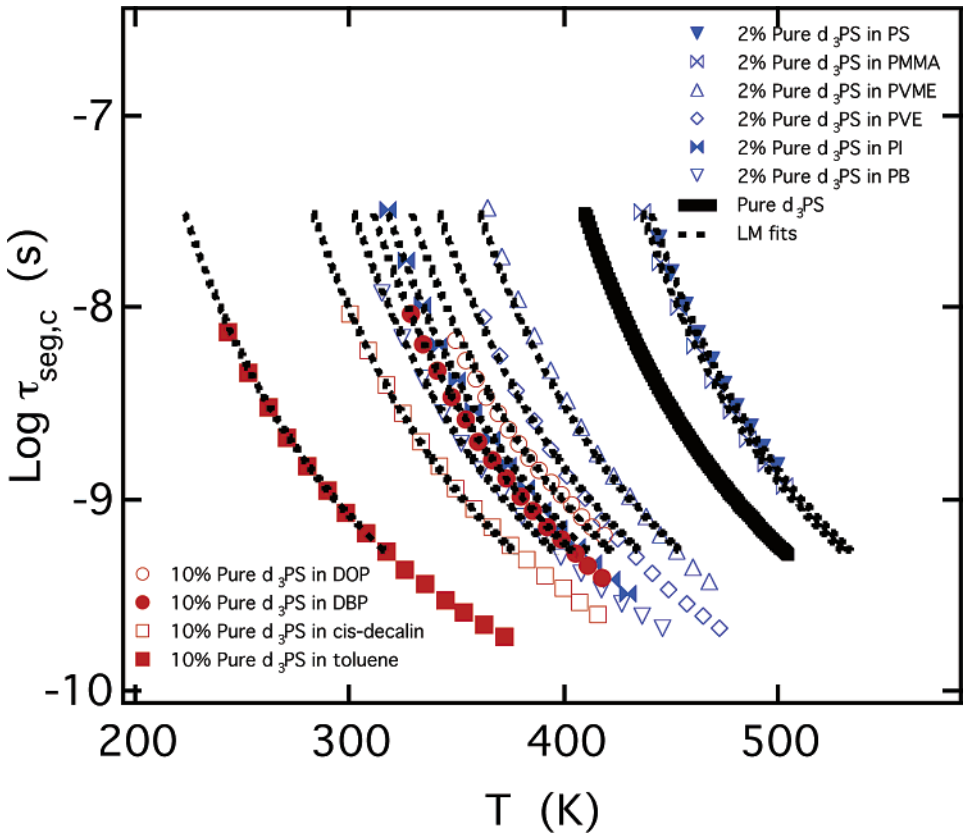

Figure 9. Lodge−McLeish fits to dilute d_3PS segmental dynamics. Dashed lines are the LM fit to 2% d_3PS dynamics in polymer hosts (blue points) and 10% d_3PS56 dynamics in solvents (red points). Fit values of ϕ_{self} can be found in Table 3.

Table 3. Self-Concentration from Lodge−McLeish Fit

blend or solution	ϕ_{self} (±0.05)
2% d_3PS/PVME	0.46
2% d_3PS/PVE	0.21
2% d_3PS/PI	0.37
2% d_3PS/PB	0.44
2% d_3PS/hPS	0.14
2% d_3PS/PMMA	
10% d_3PS56/DOP[a]	0.45
10% d_3PS56/DBP[a]	0.38
10% d_3PS56/decalin[a]	0.48
10% d_3PS56/toluene[a]	0.19

[a] Data reported in ref 54.

pure d_3PS for any value of ϕ_{self}. In contrast, we observe that the segmental dynamics of d_3PS in PMMA are about 3 times slower than pure d_3PS dynamics. For PMMA, there are a number of observations in the literature that indicate that homopolymer melt dynamics may be different than those of other vinyl polymers at the same $T - T_g$.[30,74,75]

To our knowledge, the Lodge−McLeish model has not been used quantitatively to describe polymer segmental dynamics in solution prior to this study. In work reported recently, Savin et al. presented DSC data from polymer solutions and argued that the results were qualitatively consistent with self-concentration and the LM model.[76] In particular, two T_g's were observed at intermediate compositions for one-phase polymer solutions. The work presented here indicates that the LM model can describe dilute d_3PS segmental dynamics in solvent hosts as well as it describes dynamics in polymer hosts. In a future publication, we will report on further tests of the reliability of the LM model for polymer/solvent mixtures.[77]

Utility of the Lodge−McLeish Model. Given that ϕ_{self} for d_3PS varies significantly with blending partner, one might conclude that the LM model is fundamentally unsound and practically useless. Here we argue otherwise. Our perspective is that the LM model is certainly capturing only one aspect of the change in dynamics associated with mixing (that part associated with ΔT_g). When ΔT_g is large, this part of the problem is usually dominant, and the LM model should describe the data to a reasonable approximation if the model is correct. When ΔT_g is small, it is likely that other factors related to the detailed molecular structure will play an important role. In the latter case (such as d_3PS in PMMA), the ϕ_{self} value that results from fitting data may be meaningless. Thus, we have created an alternative format for considering the experimental results that includes ΔT_g as a critical variable.

In Figure 10 we show a comparison of the segmental dynamics of polystyrene in the dilute regime in 10 different hosts (including PMMA). The abscissa shows the difference in T_g values between the polystyrene homopolymer and the host (polymer or solvent). Moving to the right indicates slower matrix dynamics. The ordinate shows $\Delta T_{g,eff}$, which is the change in dynamics (expressed as a temperature shift) for a polystyrene chain that is taken out of its pure melt and put into a host matrix as a dilute chain. Moving up indicates slower dilute chain dynamics. Also plotted in Figure 10 are four points that describe the dynamics of dilute polyisoprene chains as reported in ref 29. The general trend shown in Figure 10 is completely expected in that dilute chains move more slowly in matrices with higher glass transition temperatures. For comparison, we note that dilute chain dynamics that are completely coupled to the dynamics of the host would be represented by the

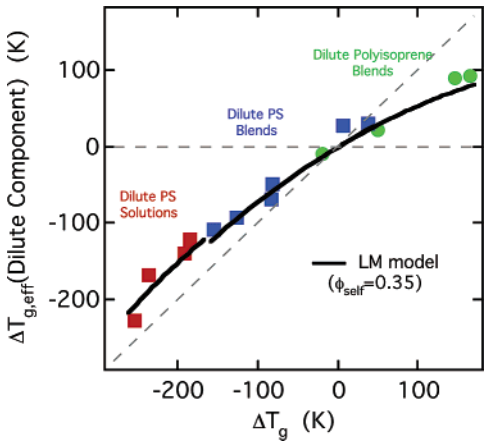

Figure 10. Dynamics of dilute polystyrene and polyisoprene chains as a function of host T_g. The vertical axis shows the temperature shift between the dilute chain's dynamics and its homopolymer melt dynamics. The horizontal axis is the difference in T_g between the host and the pure guest. Blue points are for 2% d_3PS segmental dynamics in polymer blends, red points are for 10% d_3PS segmental dynamics in solutions, and green points are for dilute PI segmental dynamics in polymer blends (ref 29). The solid black lines are the calculation of the Lodge–McLeish model with ϕ_{self} = 0.35. Two different LM lines are shown; the left corresponds to 10% composition while the right corresponds to 2%.

line of slope = 1 (ϕ_{self} = 0) in Figure 10. Dynamics that are completely independent of environment would be represented by the line of slope = 0 (ϕ_{self} = 1). The LM model with ϕ_{self} = 0.35 produces the solid lines in the figure.

Figure 10 shows that the LM model with a single value of ϕ_{self} makes useful predictions for the segmental dynamics of a large number of systems involving polystyrene or polyisoprene as dilute chains. In light of the huge temperature shifts that are observed in the systems studied (more than 200 K), a single value of ϕ_{self} = 0.35 produces results that are remarkably consistent with experimental data; the root-mean-square deviation is about 10 K, and no system (out of 14) differs from the predicted value of $T_{g,eff}$ by more than 20 K. The discrepancy between any given point and the solid curve is the result of ϕ_{self} values for that particular system being different than 0.35 (see Table 3).

We interpret Figure 10 as indicating that self-concentration plays a dominant role in determining segmental dynamics in dilute blends and that the LM model is a reasonable description of the experimental data for dilute polyisoprene and polystyrene chains. If this is "success", it is useful to specify two scenarios that would constitute "failure": (1) If the 14 data points in Figure 10 had been widely scattered rather than roughly following a single curve, that would indicate at least for these systems that the LM model could not make useful predictions based only upon homopolymer properties. (2) If the data points in Figure 10 followed the line of slope 1, that would indicate that the self-concentration effect was negligible. Interestingly, essentially this result (data following line of slope 1) is obtained if the dilute species is a rigid dye molecule as opposed to a polymer chain.[77] For a dye molecule, the self-concentration effect would be expected to be negligible.

Other Comments on the Lodge–McLeish Model. Equation 8 predicts a value of ϕ_{self} for a given polymer that is essentially independent of blending partner, temperature, and composition. We wish to comment briefly on each of these dependences.

Table 4. Self-Concentration Dependence on Composition Range

blend	ϕ_{self} from dilute blends (2–5 wt %)	ϕ_{self} from compositions of 20–80 wt %
PI in PVE	0.41 ± 0.05[29]	0.40 ± 0.05[18]
PI in PS	0.22 ± 0.05[29]	0.33 ± 0.05[23]
PS in PI	0.37 ± 0.05	0.42 ± 0.07[23]

Fits with the LM model show that ϕ_{self} depends on blending partner for dilute d_3PS in the various blends and solutions presented here (see Table 3). Figure 10 puts the significance of these variations into context.

Fits of the dilute blend data presented here with the LM model do not indicate that ϕ_{self} depends on temperature for a given blend. Recent work has suggested that the LM model is not useful for the slow component (high T_g) in miscible polymer blends.[49] In particular, ref 49 suggests ϕ_{self} will be required to vary with temperature in order to successfully describe the segmental dynamics of the slow component. The work presented here does not support this suggestion but it should be noted that the range of dynamics over which we have data (0.1–10 ns) is quite limited, and a different conclusion might be reached with data extending closer to the blend T_g.

Fits with the LM model also suggest that ϕ_{self} does not depend on composition. A summary of ϕ_{self} values determined for PI in blends with PVE and PS, as well as PS in blends with PI, is presented in Table 4. For each system, the value of ϕ_{self} determined from dilute blend measurements agrees to within experimental error of the value determined from studies at compositions ranging from 20 to 80 wt %. This agreement supports the fundamental assumption of the LM model that distinct component dynamics result from an intramolecular enrichment in local composition (self-concentration).

Effect of Dilute Chain Molecular Weight. The results reported here were obtained with relatively low molecular weight d_3PS chains that on average contain about 17 repeat units (~3 Kuhn lengths). While low molecular weight chains were selected in order to increase the number of miscible blending partners, it is reasonable to ask how this choice might have influenced our conclusions. The molecular weight dependence of ϕ_{self} is an issue that has not yet received the experimental attention that is required for a definitive answer to this question. For two miscible blend systems, it has been shown that the friction coefficients obtained for individual components are independent of molecular weight;[18,78] in both cases, chains as small as 1–2 kg/mol were utilized. For the case of polyisoprene chains in polyisoprene/polyvinylethylene, it was shown that segmental dynamics data are consistent with a ϕ_{self} value that does not depend on molecular weight, although this hypothesis was not critically tested.[18]

If the relevant length scale for blend dynamics is one Kuhn length, can these dynamics be reasonably probed by a chain of only three Kuhn lengths? The following calculation indicates that an affirmative answer is plausible. For polystyrene, the Kuhn length corresponds to about 5 repeat units; a literal interpretation of the LM model would include 2 segments on each side of a given segment as the self-concentration part of the local volume. For a chain with 17 repeat units, we would imagine that the central 13 repeat units have the self-concentration expected for a high molecular weight

chain, while the 2 units at each end have diminished self-concentration. Summing up these contributions and weighting each segment equally leads to the conclusion that a 17-mer should have an average ϕ_{self} value that is 0.93 times the value expected for a high molecular weight chain. With a ϕ_{self} of roughly 0.3, this produces a negligible difference, given our experimental error estimates. Finally, we note that the self-concentration concept has been qualitatively validated for low molecular weight chains in recent molecular dynamics computer simulations by Faller and co-workers.[35]

Conclusion

This study probed the segmental dynamics of polystyrene in miscible polymer blends in the dilute limit. Experimental results were fit with the Lodge−McLeish model and compared with model predictions. We also tested the ability of the LM model to describe d_3PS segmental dynamics in various solvents.

The LM model successfully fit the segmental dynamics of dilute d_3PS in polymer hosts of PB, PI, PVE, PVME, PMMA, and higher molecular weight PS, although different values of ϕ_{self} were required for different blending partners. The LM model also successfully fit the segmental dynamics of dilute polystyrene in four solvents. The similarity between polymer segmental dynamics in solvent and polymer hosts warrants further consideration.

While the different values of ϕ_{self} obtained for different blending partners seems contrary to the original spirit of the LM model, we propose that these differences should be considered in light of the T_g difference between the two homopolymers. When ΔT_g is small, it is reasonable that effects that are ignored in the LM development might play an equal or larger role than ΔT_g. From this perspective, the LM model with a single ϕ_{self} value reasonably describes the experimental data in dilute polystyrene and polyisoprene blends with 14 blending partners. We also showed that ϕ_{self} values determined from dilute blend studies of polystyrene and polyisoprene are consistent with the ϕ_{self} values determined from compositions ranging from 20 to 80%. This result supports the assumption of the LM model that ϕ_{self} is independent of composition.

Finally, we emphasize that our conclusions about segmental dynamics in dilute blends are limited in several important respects by lack of experimental data: (1) only dilute polystyrene and polyisoprene chains have been considered systematically, (2) in both cases low molecular weight chains were studied, (3) both studies were limited to temperatures far above the blend T_g, and (4) only the average relaxation time (not the distribution) has been considered.

Acknowledgment. This work was supported by the National Science Foundation through the Division of Material Research, Polymer Program (DMR-0355470). Some measurements were performed at the Instrument Center of the Department of Chemistry, University of Wisconsin—Madison, supported by NSF CHE-9508244 and CHE-9629688. We also thank Paul Nealey for the use of the DSC and the following for helpful comments: Ralph Colby, Sanat Kumar, Tim Lodge, and the anonymous reviewers.

Supporting Information Available: Supplementary figures presenting ^{2}H NMR spectra of neat d_3PS and 2% d_3PS in two host matrices. This material is available free of charge via the Internet at http://pubs.acs.org.

References and Notes

(1) Adachi, K.; Kotaka, T. *Macromolecules* **1985**, *18*, 466−472.
(2) Doi, M.; Edwards, S. F. *The Theory of Polymer Dynamics*; Clarendon Press: Oxford, 1988.
(3) Smith, G. D.; Paul, W.; Monkenbusch, M.; Willner, L.; Richter, D.; Qiu, X. H.; Ediger, M. D. *Macromolecules* **1999**, *32*, 8857−8865.
(4) Pathak, J. A.; Colby, R. H.; Floudas, G.; Jerome, R. *Macromolecules* **1999**, *32*, 2553−2561.
(5) Roovers, J.; Toporowski, P. M. *Macromolecules* **1992**, *25*, 3454−3461.
(6) Roovers, J.; Toporowski, P. M. *Macromolecules* **1992**, *25*, 1096−1102.
(7) Colby, R. H. *Polymer* **1989**, *30*, 1275−1278.
(8) Minnick, J. L.; Schrag, J. L. *Macromolecules* **1980**, *13*, 1690−1695.
(9) Trask, C. A.; Roland, C. M. *Macromolecules* **1989**, *22*, 256−261.
(10) Miller, J. B.; Mcgrath, K. J.; Roland, C. M.; Trask, C. A.; Garroway, A. N. *Macromolecules* **1990**, *23*, 4543−4547.
(11) Kanetakis, J.; Fytas, G.; Kremer, F.; Pakula, T. *Macromolecules* **1992**, *25*, 3484−3491.
(12) Chung, G. C.; Kornfield, J. A.; Smith, S. D. *Macromolecules* **1994**, *27*, 964−973.
(13) Adams, S.; Adolf, D. B. *Macromolecules* **1999**, *32*, 3136−3145.
(14) Zawada, J. A.; Fuller, G. G.; Colby, R. H.; Fetters, L. J.; Roovers, J. *Macromolecules* **1994**, *27*, 6861−6870.
(15) Alvarez, F.; Alegria, A.; Colmenero, J. *Macromolecules* **1997**, *30*, 597−604.
(16) Arendt, B. H.; Krishnamoorti, R.; Kornfield, J. A.; Smith, S. D. *Macromolecules* **1997**, *30*, 1127−1137.
(17) Chung, G. C.; Kornfield, J. A.; Smith, S. D. *Macromolecules* **1994**, *27*, 5729−5741.
(18) Haley, J. C.; Lodge, T. P.; He, Y. Y.; Ediger, M. D.; von Meerwall, E. D.; Mijovic, J. *Macromolecules* **2003**, *36*, 6142−6151.
(19) He, Y. Y.; Lutz, T. R.; Ediger, M. D. *Macromolecules* **2003**, *36*, 8040−8048.
(20) He, Y. Y.; Lutz, T. R.; Ediger, M. D. *Macromolecules* **2003**, *36*, 9170−9175.
(21) He, Y. Y.; Lutz, T. R.; Ediger, M. D. *J. Chem. Phys.* **2003**, *119*, 9956−9965.
(22) He, Y. Y.; Lutz, T. R.; Ediger, M. D. *Macromolecules* **2004**, *37*, 9889−9898.
(23) He, Y. Y.; Lutz, T. R.; Ediger, M. D.; Pitsikalis, M.; Hadjichristidis, N.; von Meerwall, E. D. *Macromolecules* **2005**, *38*, 6216−6226.
(24) Hoffmann, S.; Willner, L.; Richter, D.; Arbe, A.; Colmenero, J.; Farago, B. *Phys. Rev. Lett.* **2000**, *85*, 772−775.
(25) Kamath, S.; Colby, R. H.; Kumar, S. K. *Macromolecules* **2003**, *36*, 8567−8573.
(26) Kim, E.; Kramer, E. J.; Osby, J. O. *Macromolecules* **1995**, *28*, 1979−1989.
(27) Laupretre, F.; Monnerie, L.; Roovers, J. *Abstr. Pap. Am. Chem. Soc.* **2000**, *219*, U476−U476.
(28) Lutz, T. R.; He, Y. Y.; Ediger, M. D.; Cao, H. H.; Lin, G. X.; Jones, A. A. *Macromolecules* **2003**, *36*, 1724−1730.
(29) Lutz, T. R.; He, Y. Y.; Ediger, M. D.; Pitsikalis, M.; Hadjichristidis, N. *Macromolecules* **2004**, *37*, 6440−6448.
(30) Milhaupt, J. M.; Lodge, T. P.; Smith, S. D.; Hamersky, M. W. *Macromolecules* **2001**, *34*, 5561−5570.
(31) Min, B. C.; Qiu, X. H.; Ediger, M. D.; Pitsikalis, M.; Hadjichristidis, N. *Macromolecules* **2001**, *34*, 4466−4475.
(32) Salaniwal, S.; Kant, R.; Colby, R. H.; Kumar, S. K. *Macromolecules* **2002**, *35*, 9211−9218.
(33) Yang, X. P.; Halasa, A.; Hsu, W. L.; Wang, S. Q. *Macromolecules* **2001**, *34*, 8532−8540.
(34) Doxastakis, M.; Kitsiou, M.; Fytas, G.; Theodorou, D. N.; Hadjichristidis, N.; Meier, G.; Frick, B. *J. Chem. Phys.* **2000**, *112*, 8687−8694.
(35) Faller, R. *Macromolecules* **2004**, *37*, 1095−1101.
(36) Faller, R.; Reith, D. *Macromolecules* **2003**, *36*, 5406−5414.
(37) Sakai, V. G.; Chen, C. X.; Maranas, J. K. *Macromolecules* **2004**, *37*, 9975−9983.
(38) Kamath, S.; Colby, R. H.; Kumar, S. K.; Karatasos, K.; Floudas, G.; Fytas, G.; Roovers, J. E. L. *J. Chem. Phys.* **1999**, *111*, 6121−6128.
(39) Leroy, E.; Alegria, A.; Colmenero, J. *Macromolecules* **2003**, *36*, 7280−7288.

(40) Kumar, S. K.; Colby, R. H.; Anastasiadis, S. H.; Fytas, G. *J. Chem. Phys.* **1996**, *105*, 3777−3788.
(41) Lodge, T. P.; McLeish, T. C. B. *Macromolecules* **2000**, *33*, 5278−5284.
(42) Roland, C. M. *Macromolecules* **1987**, *20*, 2557−2563.
(43) Roland, C. M. *J. Polym. Sci., Part B: Polym. Phys.* **1988**, *26*, 839−856.
(44) Roland, C. M.; Ngai, K. L. *Macromolecules* **1991**, *24*, 2261−2265.
(45) Zetsche, A.; Fischer, E. W. *Acta Polym.* **1994**, *45*, 168−175.
(46) Luettmer-Strathmann, J. *J. Chem. Phys.* **2005**, *123*, Art. No. 014910.
(47) Leroy, E.; Alegria, A.; Colmenero, J. *Macromolecules* **2002**, *35*, 5587−5590.
(48) For a somewhat different perspective, see refs 49 and 50.
(49) Kant, R.; Kumar, S. K.; Colby, R. H. *Macromolecules* **2003**, *36*, 10087−10094.
(50) Krygier, E.; Lin, G. X.; Mendes, J.; Mukandela, G.; Azar, D.; Jones, A. A.; Pathak, J. A.; Colby, R. H.; Kumar, S. K.; Floudas, G.; Krishnamoorti, R.; Faust, R. *Macromolecules* **2005**, *38*, 7721−7729.
(51) Urakawa, O.; Sugihara, T.; Adachi, K. *Polym. Appl. (Jpn.)* **2002**, *51*, 10−17.
(52) Bovey, F. A. *Nuclear Magnetic Resonance Spectroscopy,* 2nd ed.; Academic Press: San Diego, CA, 1988.
(53) Jelinski, L. W. *J. Phys. Chem.* **1985**, *89*, 571−583.
(54) Zhu, W.; Ediger, M. D. *Macromolecules* **1997**, *30*, 1205−1210.
(55) Frielinghaus, H.; Schwahn, D.; Willner, L. *Macromolecules* **2001**, *34*, 1751−1763.
(56) Rizos, A. K.; Fytas, G.; Semenov, A. N. *J. Chem. Phys.* **1995**, *102*, 6931−6940.
(57) Se, K.; Takayanagi, O.; Adachi, K. *Macromolecules* **1997**, *30*, 4877−4881.
(58) Schwahn, D.; Mortensen, K.; Springer, T.; Yeemadeira, H.; Thomas, R. *J. Chem. Phys.* **1987**, *87*, 6078−6087.
(59) Wagler, T.; Rinaldi, P. L.; Han, C. D.; Chun, H. *Macromolecules* **2000**, *33*, 1778−1789.
(60) Callaghan, T. A.; Paul, D. R. *Macromolecules* **1993**, *26*, 2439−2450.
(61) Lucken, E. A. C. *Nuclear Quadrupole Coupling Constants*; Academic Press: London, 1969.
(62) Loewenstein, A. *Advances in Nuclear Quadrupole Resonance*; John Wiley & Sons: London, 1983; Vol. 5.
(63) Heatley, F. *Prog. NMR Spectrosc.* **1979**, *13*, 47−85.
(64) He, Y. Y.; Lutz, T. R.; Ediger, M. D.; Ayyagari, C.; Bedrov, D.; Smith, G. D. *Macromolecules* **2004**, *37*, 5032−5039.
(65) Tammann, G.; Hesse, W. Z. *Anorg. Allg. Chem.* **1926**, *156*, 245.
(66) Williams, M. L.; Landel, R. F.; Ferry, J. D. *J. Am. Chem. Soc.* **1955**, *77*, 3701−3707.
(67) Moe, N. E.; Qiu, X. H.; Ediger, M. D. *Macromolecules* **2000**, *33*, 2145−2152.
(68) Qiu, X. H.; Moe, N. E.; Ediger, M. D.; Fetters, L. J. *J. Chem. Phys.* **2000**, *113*, 2918−2926.
(69) Roland, C. M.; Casalini, R. *J. Chem. Phys.* **2003**, *119*, 1838−1842.
(70) T_g values used for DOP, DBP, *cis*-decalin, and toluene are 187, 179, 135, and 117 K, respectively.
(71) Temperature shifts imposed on host polymer segmental dynamics from other work based on T_g differences between polymers used in previous work and the host polymers used in this study. Temperature shifts used are −1, −13, 14 K, and no shift for pure PB, PI, PVE, and PVME, respectively.
(72) Briber, R. M.; Bauer, B. J.; Hammouda, B. *J. Chem. Phys.* **1994**, *101*, 2592−2599.
(73) Sariban, A.; Binder, K. *Makromol. Chem., Macromol. Chem. Phys.* **1988**, *189*, 2357−2365.
(74) Ferry, J. D. *Viscoelastic Properties of Polymers*, 3rd ed.; Wiley: New York, 1980.
(75) Kuebler, S. C.; Schaefer, D. J.; Boeffel, C.; Pawelzik, U.; Spiess, H. W. *Macromolecules* **1997**, *30*, 6597−6609.
(76) Savin, D. A.; Larson, A. M.; Lodge, T. P. *J. Polym. Sci., Polym. Phys.* **2004**, *42*, 1155−1163.
(77) Ediger, M. D.; Lutz, T. R.; He, Y. Y. *J. Non-Cryst. Solids*, submitted.
(78) Haley, J. C.; Lodge, T. P. *J. Chem. Phys.* **2005**, *122*, Art. No. 234914.

MA0513113